



PARAMETRIC STUDY FOR AN EFFICIENT MESHLESS METHOD IN VIBRATION ANALYSIS

Y. H. WANG AND W. D. LI

Department of Civil Engineering, Huazhong University of Science and Technology, Wuhan, Hubei, 430074, People's Republic of China

AND

L. G. THAM, P. K. K. LEE AND Z. Q. YUE

Department of Civil Engineering, The University of Hong Kong, Hong Kong, People's Republic of China

(Received 26 January 2001, and in final form 5 November 2001)

Based on the moving least-squares (MLS) approach, an efficient meshless method is employed to generate the displacement functions for vibration analysis of elastic bodies. The equation of motion is established by following the standard procedure and the boundary conditions are imposed by applying penalty functions. As the displacement functions are expressed in terms of weight functions, the accuracy will depend on the parameters of the weight functions. Therefore, a parametric study is carried out to determine the best values for these parameters. To demonstrate the accuracy, modal analyses of the beams and plates with different boundaries have been carried out. In addition, the responses of these structures under dynamic excitation have been analyzed. The examples include simply supported beams subjected to sudden excitations and simply supported plates subjected to initial displacements.

© 2002 Elsevier Science Ltd. All rights reserved.

1. INTRODUCTION

Meshless method has been developed rapidly in the last 20 years [1–13]. The method is attractive because it does not require element connectivity information. Therefore, it has the following advantages: (1) it does not require mesh data; (2) one only has to consider nodal displacements and boundary conditions; (3) compatibility is satisfied automatically as the field functions and their gradients are continuous.

The meshless method has found applications in both static as well as dynamic stress analyses. Applications in static analyses include fracture problems [2, 4, 14–17], bending of beams, plates and shells [4, 18–20], three-dimensional stress analyses [4, 17, 21, 22], contact problems [23, 24] and large deformation [5, 13, 24–27]. For dynamic analysis, Lu *et al.* [28] extended element-free Galerkin method for wave propagation and dynamic fracture. Nagashima [29] used a node-by-node meshless approach to solve the eigenvalue problem of structural vibration. Liu *et al.* [30] proposed the reproducing kernel particle methods for free vibration of beams and plates. Ouatouati *et al.* [31] developed an approach for integrating the boundary conditions using the concept of intermediate structure to solve modal analysis problems.

One of the major difficulties in the implementation of the meshless methods is how to impose the boundary conditions. Zhang *et al.* [32] have carried out a detailed study on

various schemes, namely direct collocation method, Lagrange multiple approach, modified variational principles, penalty methods and coupling finite element, and assessed the advantages of the various schemes. It has been concluded that the penalty method is simple and it can give accurate results if appropriate penalty functions are chosen. In this paper, vibration problems are analyzed further by the meshless method based on the moving least-squares approach. The equation of motion of the system is obtained by following the standard procedures and penalty functions are used to impose the essential boundary conditions. An advantage of this method is that the stiffness matrix remains symmetric and positive-definite. In addition, the number of unknowns in the solution equations will not be increased. As the accuracy of the method depends on the parameters of the weight functions, parametric study has been carried out to determine their best values. Benchmark examples, including free vibration and forced vibration of beams and plates, are analyzed to demonstrate the validity and versatility of the method. The results obtained are in good agreement with the analytical solutions.

2. MOVING LEAST-SQUARES METHOD APPROACH

One can express the approximate displacements of $u(\mathbf{x})$ in the domain Ω as $u^h(\mathbf{x})$ [4, 19, 33]:

$$u^h(\mathbf{x}) = \sum_{j=1}^m p_j(\mathbf{x}) a_j(\mathbf{x}) = \mathbf{p}^T(\mathbf{x}) \mathbf{a}(\mathbf{x}), \quad (1)$$

where $\mathbf{a}(\mathbf{x})$ are coefficients, which are functions of the spatial co-ordinates \mathbf{x} , $\mathbf{p}(\mathbf{x})$ are complete polynomials, m is the number of terms of the polynomials. In the present study, linear and quadratic polynomials are chosen for two-dimensional plane stress/strain and plate bending problems, respectively, that is

$$\begin{aligned} \mathbf{p}^T(\mathbf{x}) &= [1 \ x \ y], \quad m = 3, \\ \mathbf{p}^T(\mathbf{x}) &= [1 \ x \ y \ x^2 \ xy \ y^2], \quad m = 6. \end{aligned} \quad (2)$$

The local approximation of $u^h(\mathbf{x})$ can be written as [2]

$$u^h(\mathbf{x}) = \sum_{j=1}^m p_j(\mathbf{x}^*) a_j(\mathbf{x}) = \mathbf{p}^T(\mathbf{x}^*) \mathbf{a}(\mathbf{x}), \quad (3)$$

where \mathbf{x}^* represents the approximate of \mathbf{x} in the local subdomain. It can be shown readily that the solution of the displacement function can be obtained by carrying out least-squares fit for the local approximation of the displacement function, that is

$$\begin{aligned} J &= \sum_{j=1}^n w(\|\mathbf{x} - \mathbf{x}_j\|) [u^h(\mathbf{x}, \mathbf{x}_j) - u(\mathbf{x}_j)]^2 \\ &= \sum_{j=1}^n w(\|\mathbf{x} - \mathbf{x}_j\|) \left[\sum_{i=1}^m p_i(\mathbf{x}_j) a_i(\mathbf{x}) - u^*(\mathbf{x}_j) \right]^2, \end{aligned} \quad (4)$$

where $w(\|\mathbf{x} - \mathbf{x}_j\|)$ are the weight functions, \mathbf{x}_j are the co-ordinates of the j th node in the domain of influence of \mathbf{x} , $u^*(\mathbf{x}_j)$ are the displacements at node \mathbf{x}_j .

Minimizing J with respect to a_i , we have

$$\partial J / \partial a_i = 0. \quad (5)$$

One can show readily that

$$\mathbf{a}(\mathbf{x}) = \mathbf{A}^{-1}(\mathbf{x}) \mathbf{B}(\mathbf{x}) \mathbf{u}^*, \quad (6)$$

where $\mathbf{A}(\mathbf{x})$ is an $m \times m$ matrix, $\mathbf{B}(\mathbf{x})$ is an $m \times n$ matrix, \mathbf{u}^* is an n -column vector. They are defined as follows:

$$\mathbf{A}(\mathbf{x}) = \sum_i^n w(\|\mathbf{x} - \mathbf{x}_i\|) \mathbf{p}(\mathbf{x}_i) \mathbf{p}^T(\mathbf{x}_i), \tag{7a}$$

$$\mathbf{B}(\mathbf{x}) = [w(\|\mathbf{x} - \mathbf{x}_1\|)p(\mathbf{x}_1) \cdots w(\|\mathbf{x} - \mathbf{x}_n\|)p(\mathbf{x}_n)], \tag{7b}$$

$$\mathbf{u}^* = [u_1^*, u_2^* \cdots u_n^*]^T. \tag{7c}$$

Substituting equations (7a-7c) into equation (1), we can obtain

$$u^h(\mathbf{x}) = \sum_i^n \sum_j^m p_j(\mathbf{x})(\mathbf{A}^{-1}(\mathbf{x})\mathbf{B}(\mathbf{x}))_{ji}u_i = \sum_i^n \varphi_i(\mathbf{x})\mathbf{u}_i^*, \tag{8}$$

$$\varphi_i(\mathbf{x}) = \sum_j^m p_j(\mathbf{x})(\mathbf{A}^{-1}(\mathbf{x})\mathbf{B}(\mathbf{x}))_{ji}, \tag{9}$$

where $\varphi_i(\mathbf{x})$ represents the values of the shape function of node i at point \mathbf{x} .

The partial derivatives of $\varphi_i(\mathbf{x})$ can be defined as follows:

$$\varphi_{i,k} = \sum_j^m \{p_{j,k}(\mathbf{A}^{-1}\mathbf{B})_{ji} + p_j(\mathbf{A}_{,k}^{-1}\mathbf{B} + \mathbf{A}^{-1}\mathbf{B}_{,k})_{ji}\}, \tag{10}$$

where

$$\mathbf{A}_{,k}^{-1} = -\mathbf{A}^{-1}\mathbf{A}_{,k}\mathbf{A}^{-1}. \tag{11}$$

3. WEIGHT FUNCTIONS

It is obvious that the weight functions, $w(\|\mathbf{x} - \mathbf{x}_j\|)$, will play an important role in the performance of the method, and therefore, they must be chosen carefully. Such functions should satisfy the following criteria [4]:

- (1) they must be of compact support;
- (2) they must not be negative over its support;
- (3) they should decrease in magnitude as the distance from \mathbf{x} to \mathbf{x}_j increases;
- (4) their first and second partial derivatives must be non-singular.

In this paper, the weight functions are chosen as

$$w(d_i) = \begin{cases} \frac{e^{-(d_i/c)^k} - e^{-(d_m/c)^k}}{1 - e^{-(d_m/c)^k}}, & d_i \leq d_m, \\ 0 & d_i > d_m, \end{cases} \tag{12}$$

where $d_i = \|\mathbf{x} - \mathbf{x}_i\|$ is the distance between the two points \mathbf{x} and \mathbf{x}_i (Figure 1). Note that point i is the center of the cell. For uniformly distributed nodes, c_i is the maximum distance between point i and other nodes in the cell. As recommended by Belytschko *et al.* [34],

$$c_i = \max_{j \in S_j} \|\mathbf{x}_j - \mathbf{x}_i\|, \tag{13}$$

where S_j is the minimum set of points \mathbf{x}_i that construct a polygon in the neighborhood of the point \mathbf{x}_i . c is a constant that controls the relative weights and is defined as follows:

$$c = \lambda c_i,$$

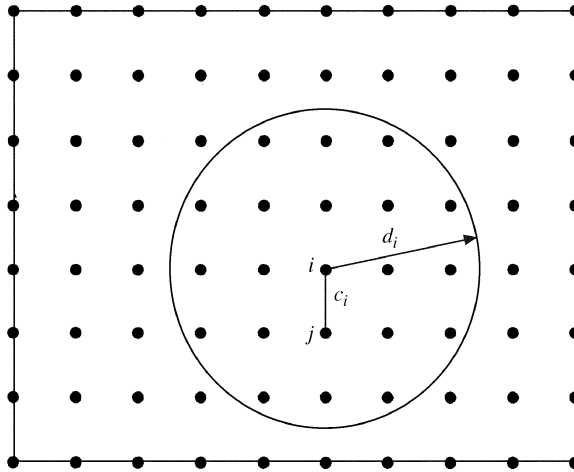


Figure 1. Illustration of the domain of influence.

where $\lambda (= c/c_i)$ is a multiplying parameter, whose best value can be determined numerically.

In equation (12), d_m is the size of the support for the weight function $w(d_i)$ and determines the domain influence of node \mathbf{x}_i . The value should be chosen to ensure that the inverse of the matrix \mathbf{A} in equation (6) exists. If it is too small, the inverse matrix may not exist. On the other hand, the computer time taken will be very long if d_m is large. Parametric study will be carried out to determine the optimum values for d_m . It may be pointed that the present method does not need any kind of “background” or shadow mesh for integration.

In equation (12), k is another parameter determining the influence of the weight functions and its best value will be determined numerically in section 6.

4. DYNAMIC EQUATIONS

4.1. TWO-DIMENSIONAL ELASTIC BODY

The equation of motion for a structure is [35]

$$\mathbf{M}\ddot{\mathbf{u}}(t) + \mathbf{C}\dot{\mathbf{u}}(t) + \mathbf{K}\mathbf{u}(t) = \mathbf{F}(t), \tag{14}$$

where $\ddot{\mathbf{u}}(t)$, $\dot{\mathbf{u}}(t)$ and $\mathbf{u}(t)$ are the vectors of displacements, velocities and accelerations, respectively, \mathbf{M} is the mass matrix, \mathbf{C} is the damping matrix, and \mathbf{K} is the stiffness matrix. According to the equilibrium equations and boundary conditions of the elastic body, the energy function can be obtained. Minimizing the energy function and imposing the boundary conditions by adopting the penalty method, the stiffness matrix can be written as [36]

$$\mathbf{K} = \int_{\Omega} \mathbf{B}^T \mathbf{D} \mathbf{B} \, d\Omega + \int_{\Gamma_u} \alpha \boldsymbol{\varphi}^T \mathbf{Q} \boldsymbol{\varphi} \, d\Gamma, \tag{15}$$

where

$$\mathbf{Q} = \begin{bmatrix} \cos^2 \theta & \sin \theta \cos \theta \\ \sin \theta \cos \theta & \sin^2 \theta \end{bmatrix}$$

in which θ is the angle between the boundary Γ_u and the positive direction of the x -axis.

In equation (15), $\boldsymbol{\varphi}$ is the shape function matrix for an n -degree problem

$$\boldsymbol{\varphi} = \begin{bmatrix} \varphi_1 & 0 & \varphi_2 & 0 & \cdots & \varphi_n & 0 \\ 0 & \varphi_1 & 0 & \varphi_2 & \cdots & 0 & \varphi_n \end{bmatrix}, \tag{16}$$

\mathbf{B} is the strain martrix

$$\mathbf{B} = \begin{bmatrix} \varphi_{1,x} & 0 & \varphi_{2,x} & 0 & \cdots & \varphi_{n,x} & 0 \\ 0 & \varphi_{1,y} & 0 & \varphi_{2,y} & \cdots & 0 & \varphi_{n,y} \\ \varphi_{1,y} & \varphi_{1,x} & \varphi_{2,y} & \varphi_{2,x} & \cdots & \varphi_{n,y} & \varphi_{n,x} \end{bmatrix}, \tag{17}$$

\mathbf{D} is the elastic matrix. For plane stress problem,

$$\mathbf{D} = \frac{E}{1 - \mu^2} \begin{bmatrix} 1 & \mu & 0 \\ \mu & 1 & 0 \\ 0 & 0 & \frac{1 - \mu}{2} \end{bmatrix}. \tag{18}$$

For plane strain problem, one can replace E by $E/(1 - \mu^2)$, μ by $\mu/(1 - \mu)$ in equation (18). The penalty parameter must be chosen in such a way that the main component of the second term of equation (15) is greater than the first term and such choice will ensure that the boundary conditions will be satisfied and the stiffness matrix will not be singular. In this study, α is taken to be $2.0 \times 10^3 E$, in which E is the modulus of elasticity.

The mass matrix \mathbf{M} can be calculated by

$$\mathbf{M} = \int_{\Omega} \rho \boldsymbol{\varphi}^T \boldsymbol{\varphi} \, d\Omega, \tag{19}$$

where ρ is the density of the material.

The damping matrix \mathbf{C} can be expressed as a linear combination of mass and stiffness matrices as

$$\mathbf{C} = \beta_1 \mathbf{M} + \beta_2 \mathbf{K}, \tag{20}$$

where β_1 and β_2 are constants.

It can be shown readily that the loading vector $\mathbf{F}(t)$ can be written as [19]

$$\mathbf{F}(t) = \int_{\Omega} \boldsymbol{\varphi}^T \mathbf{b} \, d\Omega + \int_{\Gamma_f} \boldsymbol{\varphi}^T \mathbf{f}(t) \, d\Gamma + \alpha \int_{\Gamma_u} \bar{\mathbf{u}} \boldsymbol{\varphi}^T \mathbf{Q} \mathbf{q} \, d\Gamma + \sum_{n=1}^{n_c} \boldsymbol{\varphi}^T(\mathbf{x}_n) \mathbf{T}_n(\mathbf{x}_n, t), \tag{21}$$

where \mathbf{b} is the body force vector, $\mathbf{f}(t)$ is the surface forces acting on the boundary Γ_f of the elastic body at time t , $\bar{\mathbf{u}}$ is the prescribed displacement vector on the boundary Γ_u , $\mathbf{T}_n(\mathbf{x}_n, t)$ is the n th concentrate force acting on the elastic body at \mathbf{x}_n and at time t , and

$$\mathbf{q} = \begin{pmatrix} \cos \theta \\ \sin \theta \end{pmatrix}.$$

4.2. BENDING OF PLATE

The stiffness matrix of the bending plate is

$$\mathbf{K} = \int_{\Omega} \mathbf{B}^T \mathbf{D} \mathbf{B} \, d\Omega + \alpha \left(\int_{\Gamma_1} \boldsymbol{\varphi}^T \boldsymbol{\varphi} \, d\Gamma + \int_{\Gamma_2} \boldsymbol{\varphi}_{,n}^T \boldsymbol{\varphi}_{,n} \, d\Gamma \right), \tag{22}$$

where Γ_1 and Γ_2 are the simply supported and clamped boundaries respectively.

For plate bending problems, α in equation (22) is the same as in equation (15). Note that the expressions of the mass and damping matrices have the same forms as equations (19) and (20).

In equation (22), $\boldsymbol{\varphi}$ is the shape function matrix for an n -degree problem as

$$\boldsymbol{\varphi} = [\varphi_1 \quad \varphi_2 \quad \cdots \quad \varphi_n], \quad (23)$$

$$\mathbf{B} = \begin{bmatrix} -\varphi_{1,xx} & -\varphi_{2,xx} & \cdots & -\varphi_{n,xx} \\ -\varphi_{1,yy} & -\varphi_{2,yy} & \cdots & -\varphi_{n,yy} \\ -2\varphi_{1,xy} & -2\varphi_{2,xy} & \cdots & -2\varphi_{n,xy} \end{bmatrix}, \quad (24)$$

$$\mathbf{D} = D_0 \begin{bmatrix} 1 & \mu & 0 \\ \mu & 1 & 0 \\ 0 & 0 & \frac{1-\mu}{2} \end{bmatrix}, \quad (25)$$

where D_0 is the flexural rigidity of the plate, and $D_0 = Eh^3/12(1 - \mu^2)$, in which h is the thickness of the plate.

The loading vector of the plate can be shown to be

$$\mathbf{F}(t) = \int_{\Omega} \boldsymbol{\varphi}^T \mathbf{b} \, d\Omega + \int_{\Omega} \boldsymbol{\varphi}^T q(t) \, d\Omega + \sum_{n=1}^{n_c} \boldsymbol{\varphi}^T(\mathbf{x}_n) \mathbf{T}_n(\mathbf{x}_n, t), \quad (26)$$

where $q(t)$ is the transverse load per unit of the plate. Other symbols are the same as in equation (21).

5. DYNAMIC ANALYSIS

5.1. FREE VIBRATION ANALYSIS

If the damping is neglected and the external forces are zero, equation (14) will degenerate into the free vibration equation

$$\mathbf{M}\ddot{\mathbf{u}}(t) + \mathbf{K}\mathbf{u}(t) = 0. \quad (27)$$

The solutions of the above equation can be obtained by assuming

$$\mathbf{u}(t) = \mathbf{X} \sin \omega(t - t_0), \quad (28)$$

where \mathbf{X} is the mode shape representing the amplitudes of the displacements, $\mathbf{u}(t)$, ω denotes the natural frequencies of vibration, t_0 is a constant determined by the initial conditions.

By substituting equation (28) into equation (27), we have

$$\mathbf{K}\mathbf{X} - \omega^2 \mathbf{M}\mathbf{X} = 0. \quad (29)$$

In the present study, the subspace iteration method is used to solve the eigenvalue problem defined by equation (29).

5.2. FORCED VIBRATION RESPONSE

For forced vibration analysis, the solution of equation (14) can be obtained, in general, by two methods: mode superposition and direct integration. In the present study, the latter

TABLE 1
Parameters adopted in the analysis

	Cantilever beam	Square plate	Circular plate
Material parameters			
E	20.0 GPa	20.0 GPa	20.0 GPa
μ	0.3	0.3	0.3
ρ	$3.0 \times 10^3 \text{ kg/m}^3$	$3.0 \times 10^3 \text{ kg/m}^3$	$3.0 \times 10^3 \text{ kg/m}^3$
Geometrical parameters	Length $l = 40 \text{ m}$ Height $h = 0.8 \text{ m}$ Width $w = 0.4 \text{ m}$	Length $a = 4 \text{ m}$ Thickness $h = 0.2 \text{ m}$	Radius $a = 2 \text{ m}$ Thickness $h = 0.2 \text{ m}$
Computation parameters			
Number of cells	80	100	100
Number of nodes	123	121	81

approach is adopted as it is more suitable for the dynamic problem with large number of degrees of freedom. It involves the numerical integration of the equation of motion by marching in a series of time steps Δt using Wilson \mathcal{G} method. Accelerations, velocities and displacements at each step can be evaluated accordingly. As the algorithm is well documented in standard textbooks [35, 37], readers may refer to them for details of the method.

6. EXAMPLES FOR MODAL ANALYSIS

As the accuracy of the results is effected by the choice of parameters of the weight functions, a parametric study is carried out on these parameters, that is k , c/c_i and d_m/c_i . The influence of the parameters on the accuracy of the results for different structures including the cantilever beams, square and circular plates is assessed. The geometry and material constants of the beams and plates as well as other pertinent parameters used in the analyses are given in Table 1.

6.1. PARAMETERS c/c_i AND d_m/c_i

In the first case, k is kept to be constant and $= 2$. c_i is 1.0 and 0.4 m for the beam and plate respectively. Varying c and d_m , the first eight frequencies are computed. Figures 2-4 show the variations of the non-dimensional frequencies ($\omega \sqrt{ml^4/EI}$ for the beam, $\omega \sqrt{\rho a^4 h/D_0}$ for the plate, where m is the beam mass of unit length, I is the area moment of inertia of the cross-section, ρ is the plate mass of unit area) with c/c_i and d_m/c_i for different structures, that is, beams, square and circular plates. From the figures, one can conclude that the frequencies converge rapidly when $c/c_i \geq 1.0$ and $d_m/c_i \geq 4.0$. The results also confirm that the computed frequencies agree very well with the analytical solutions.

6.2. PARAMETER k

In order to study the influence of k , c/c_i and d_m/c_i are assumed to be 1.0 and 4.0 respectively. Figures 5-7 show the variations of the non-dimensional frequencies with k for the cantilever beam and simply supported plates. In the figures, the horizontal line

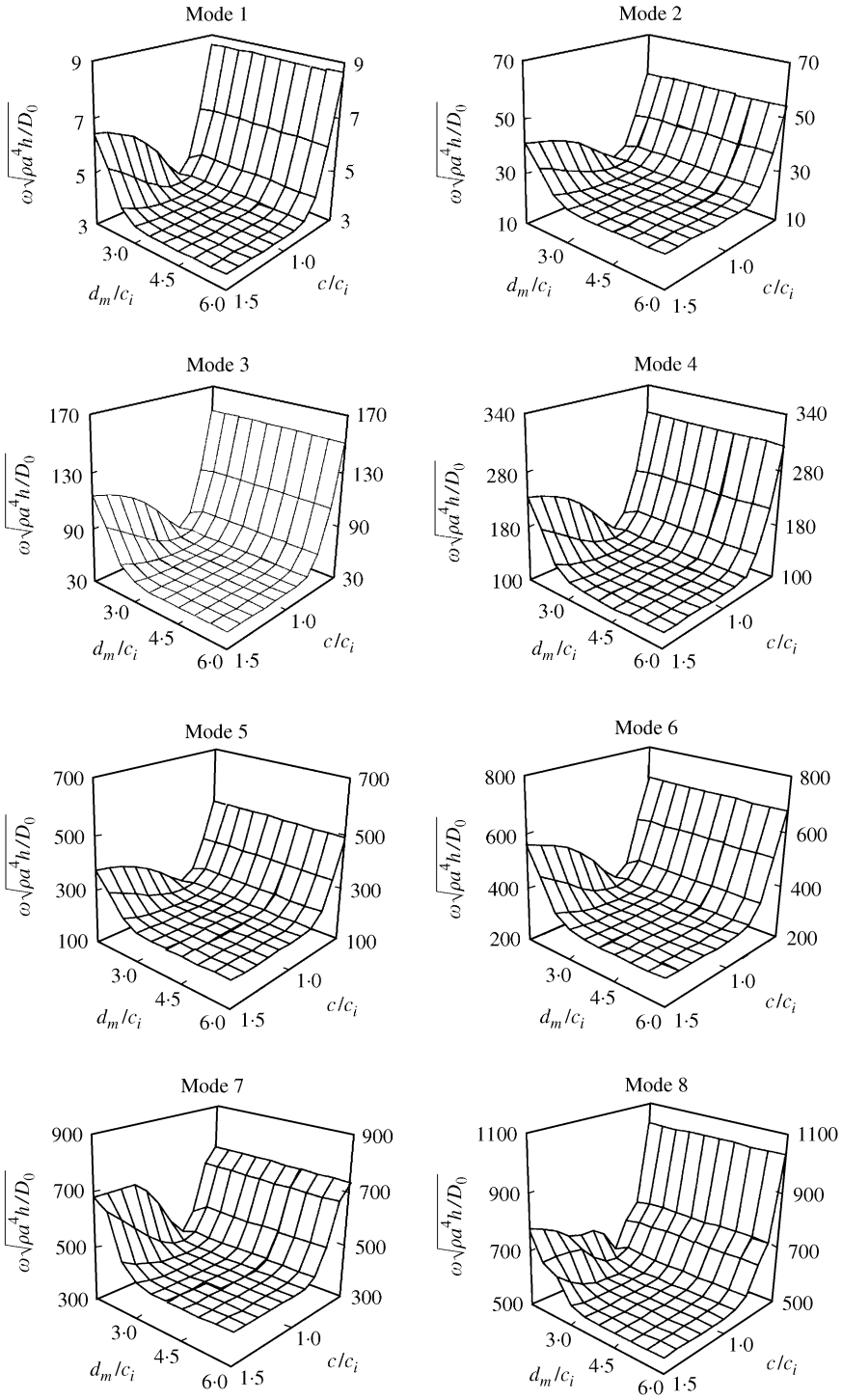


Figure 2. Influence of c/c_i and d_m/c_i on the frequencies of the cantilever ($k = 2$).

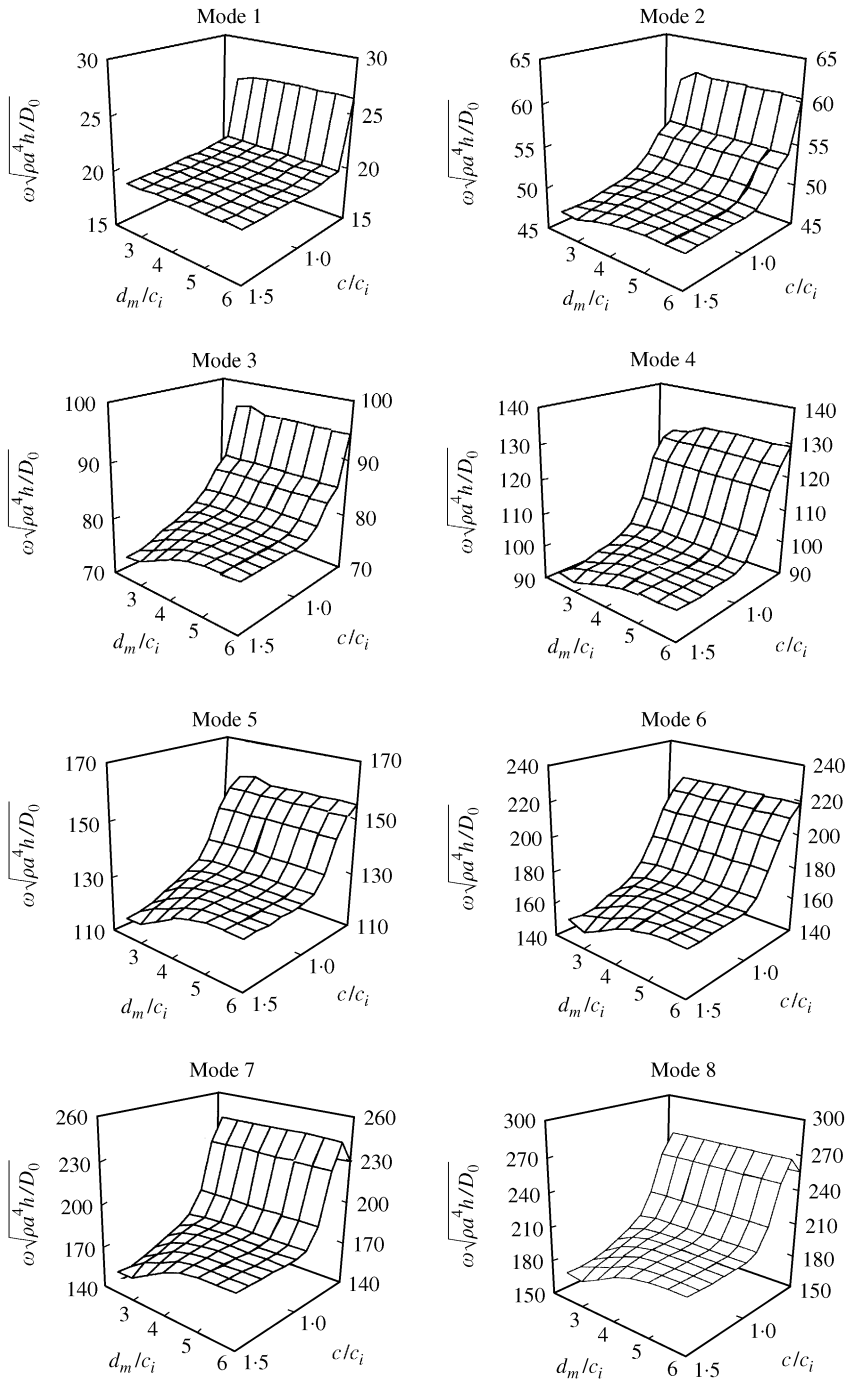


Figure 3. Influence of c/c_i and d_m/c_i on the frequencies of the simply supported square plate ($k = 2$).

represents the analytical solutions. One may conclude from the results and k has considerable influence on the frequencies results. When $k \approx 2$, the curves attain minimum values of frequencies. Such observations are different from those in reference [31]. In Figure 5 of reference [31], the frequency curves of the beam have no minimum. The analytical

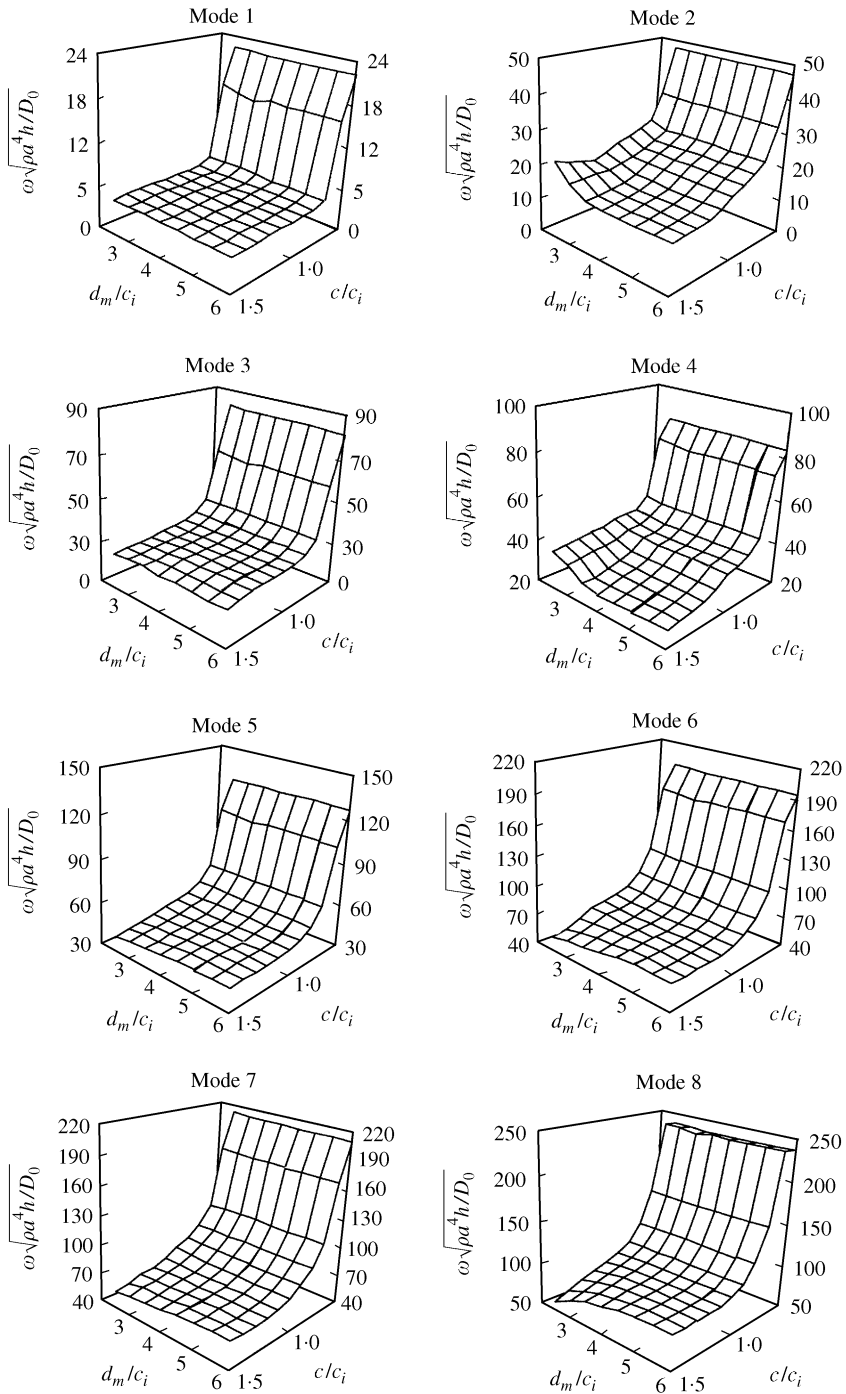


Figure 4. Influence of c/c_i and d_m/c_i on the frequencies of the simply supported circular plate ($k = 2$).

solution, which is represented by the horizontal line, intersects the curve at $k = 2$. On the other hand, the analytical solution of the plates intersects the numerical solution at two points with $k \simeq 2$ and 5 (Figure 8 of reference [31]). Therefore, k does not correspond to the minimum of the curve.

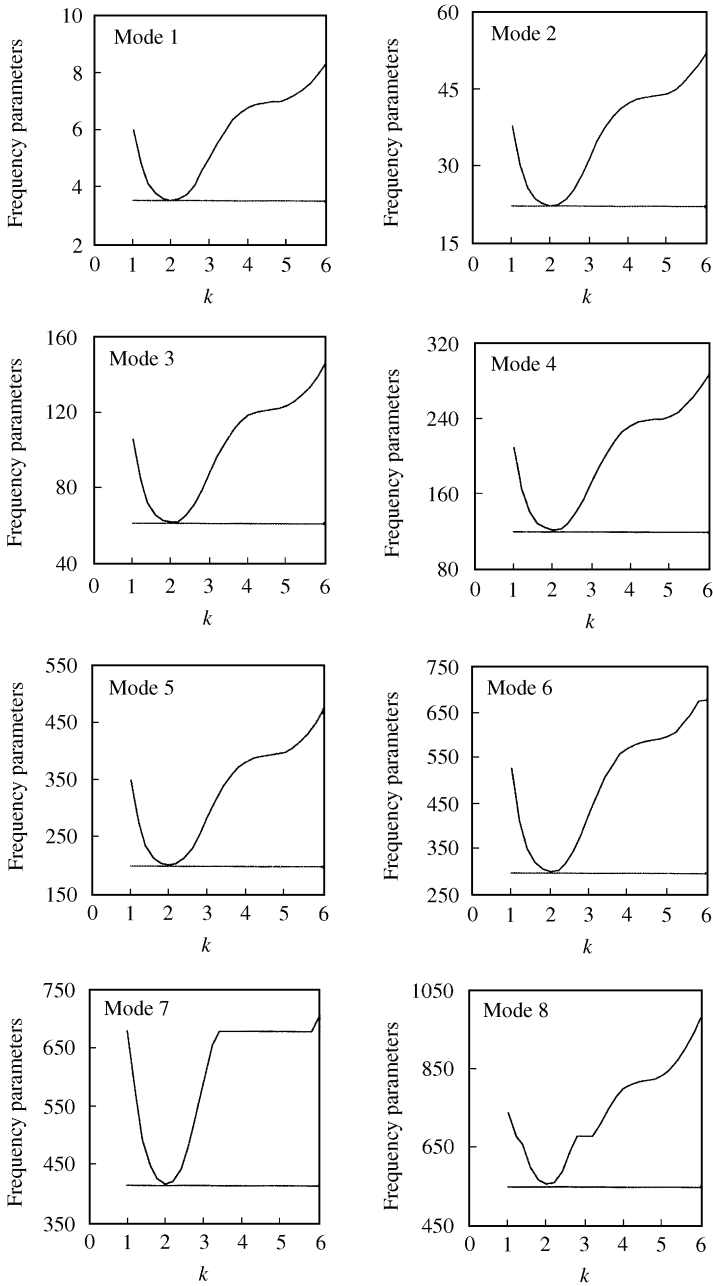


Figure 5. Influence of k on the frequencies of the cantilever ($c/c_i = 1.0$, $d_m/c_i = 4.0$).

Compared with reference [31], the present method gives a direct way for determining k . For a frequency— k curve, the minimum of the curve corresponds to the exact solution. This is important for the cases when the analytical solution is not available early.

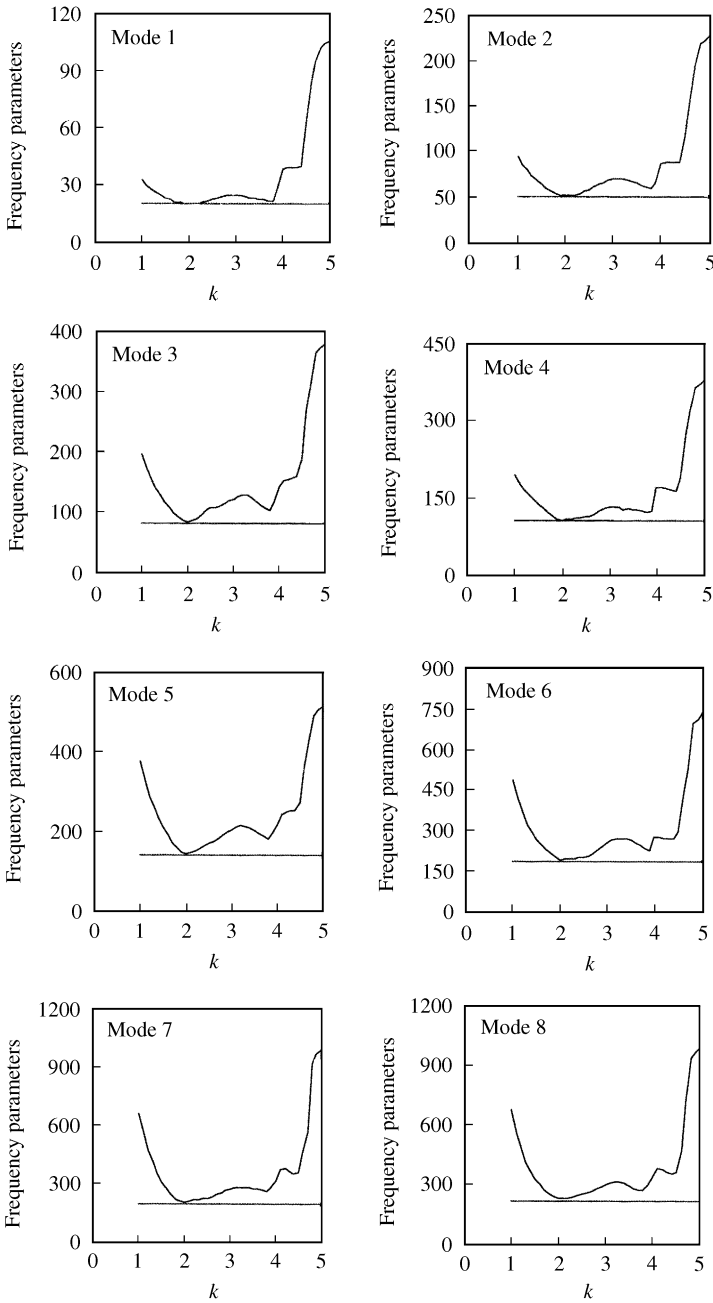


Figure 6. Influence of k on the frequencies of the simply supported square plate ($c/c_i = 1.0$, $d_m/c_i = 4.0$).

6.3. RESULTS FOR DIFFERENT BOUNDARIES

In order to examine the influence of the boundaries, beams and plates with different supports have been considered. According to the above analysis, the following values are taken for the parameters: $k = 2$, $c/c_i = 1.0$, $d_m/c_i = 4.0$.

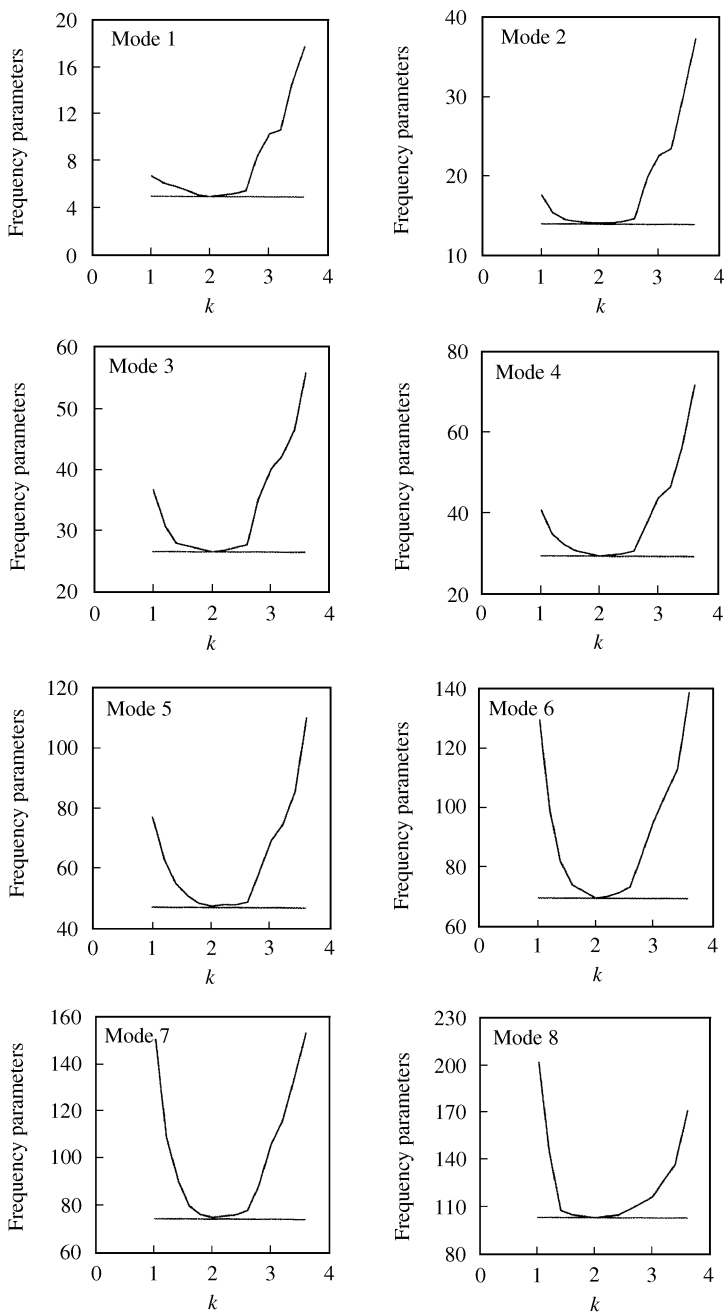


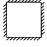
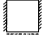



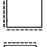

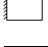
Figure 7. Influence of k on the frequencies of the simply supported circular plate ($c/c_i = 1.0$, $d_m/c_i = 4.0$).

Tables 2–4 show the frequencies for the beams, square and circular plates with different boundaries. Both analytical solutions [38, 39] and present results are listed. From the tables, it can be seen that the present method can yield accurate results.

TABLE 2
Non-dimensional frequencies of beams

Mode	Boundary conditions							
	Beam C-F		Beam C-C		Beam C-S		Beam S-S	
	Meshless method	Analytical method	Meshless method	Analytical method	Meshless method	Analytical method	Meshless method	Analytical method
1	3.526	3.516	22.637	22.374	15.512	15.416	9.871	9.870
2	22.168	22.039	62.419	61.675	50.260	49.970	39.472	39.478
3	62.058	61.695	122.352	120.903	104.837	104.253	88.772	88.826
4	121.568	120.903	202.201	199.860	179.211	178.270	157.731	157.914
5	200.873	199.859	301.934	298.556	273.303	272.031	246.270	246.740
6	299.872	298.556	421.473	416.991	387.046	385.531	354.309	355.306
7	418.497	416.991	560.740	555.165	520.354	518.771	481.752	483.611
8	556.651	555.165	719.639	713.308	673.114	671.750	628.469	631.655

TABLE 3
Non-dimensional values of the first six frequencies of square plates

Boundary	Methods	Frequency					
		1	2	3	4	5	6
	Present	36.120	73.631	108.521	132.743	165.569	243.790
	Analytical	35.988	73.393	108.160	132.250	164.866	243.148
	Present	29.026	54.936	69.850	95.276	102.798	130.917
	Analytical	28.944	54.745	69.322	94.576	102.212	129.050
	Present	23.674	51.790	58.876	86.449	100.756	114.225
	Analytical	23.649	51.667	58.645	86.118	100.200	113.210
	Present	19.738	49.379	78.948	98.920	128.374	168.484
	Analytical	19.739	49.348	78.957	98.696	128.369	167.703
	Present	12.695	33.119	41.817	63.190	72.675	91.150
	Analytical	12.688	33.063	41.693	63.012	72.403	90.611
	Present	11.691	27.758	41.304	59.149	61.942	90.820
	Analytical	11.683	27.762	41.204	59.075	61.858	90.288
	Present	9.638	16.143	36.719	39.055	46.850	70.813
	Analytical	9.629	16.128	36.724	38.938	46.745	70.745
	Present	3.472	8.548	21.319	27.225	31.036	54.359
	Analytical	3.474	8.591	21.298	27.154	31.036	54.178

7. FORCED VIBRATION

Another important subject in vibration is the response of the system to external forces and (or) initial displacements and the meshless method is also used to obtain the solutions for two different excitation cases.

7.1. CANTILEVER BEAM WITH A SUDDENLY APPLIED LOAD

A simply supported beam having the same geometry, material parameters as given in the previous section is studied. A loading $P = 10 \text{ kN/m}$ is applied suddenly at the center of the

TABLE 4

Non-dimensional frequencies of circular plates

Boundary condition	Method	Frequency							
		1	2	3	4	5	6	7	8
Fixed	Present	10.301	21.451	35.038	40.319	61.207	84.981	89.645	120.982
	Analytical	10.214	21.271	34.869	39.766	60.824	84.622	89.076	120.122
Simply supported	Present	5.002	14.017	25.813	30.011	48.838	70.596	74.613	104.092
	Analytical	4.977	13.943	25.654	29.757	48.511	70.141	74.184	103.023

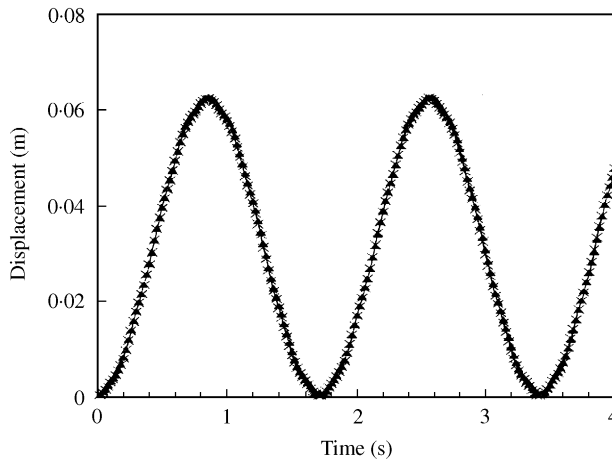


Figure 8. Displacement at the center of the simply supported beam. ▲ The proposed method; × exact solution.

beam. The displacement, velocity and acceleration at the center of the beam can be obtained analytically [40]

$$\begin{aligned}
 u\left(\frac{l}{2}, t\right) &= \frac{2Pl^3}{\pi^4 EI} \left(\frac{1 - \cos \omega_1 t}{1} + \frac{1 - \cos \omega_3 t}{81} + \frac{1 - \cos \omega_5 t}{625} + \dots \right), \\
 \dot{u}\left(\frac{l}{2}, t\right) &= \frac{2Pl^3}{\pi^4 EI} \left(\frac{\omega_1 \sin \omega_1 t}{1} + \frac{\omega_3 \sin \omega_3 t}{81} + \frac{\omega_5 \sin \omega_5 t}{625} + \dots \right), \\
 \ddot{u}\left(\frac{l}{2}, t\right) &= \frac{2Pl^3}{\pi^4 EI} \left(\frac{\omega_1^2 \cos \omega_1 t}{1} + \frac{\omega_3^2 \cos \omega_3 t}{81} + \frac{\omega_5^2 \cos \omega_5 t}{625} + \dots \right).
 \end{aligned}
 \tag{30}$$

In the meshless method, Wilson \mathcal{G} method is applied to solve the dynamic differential equations. To obtain a stable solution, \mathcal{G} is taken to be 1.4, and the time increment $\Delta t = 0.002$ s.

Figures 8–10 show the variations of the displacement, velocity and acceleration at the center of the beam obtained by the proposed method. The analytical solutions are also presented in the figures. One can conclude that the results obtained by the two methods agree very well with each other.

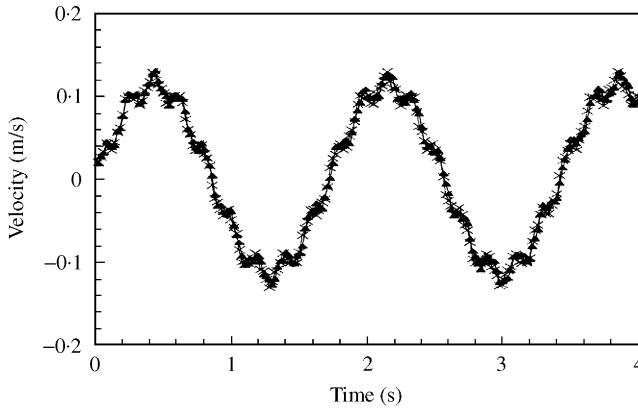


Figure 9. Velocity at the center of the simply supported beam. ▲ The proposed method; × exact solution.

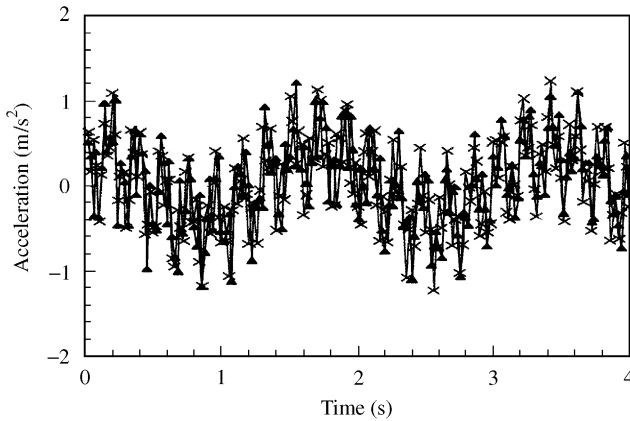


Figure 10. Acceleration at the center of the simply supported beam. ▲ The proposed method; × exact solution.

7.2. SIMPLY SUPPORTED SQUARE PLATE WITH AN INITIAL DEFLECTION

The second example deals with the dynamic response of a simply supported square plate subjected to an initial excitation. The geometrical and material parameters of the plate are given in Table 1. The initial deflection is $w_0(x, y) = 0.01 \sin \pi x/a \sin \pi y/b$. The initial velocity and acceleration are zero. The analytical solutions for the deflection, velocity and acceleration at the square center are [41]

$$\begin{aligned}
 w(t) &= 0.01 \cos \left[\pi^2 \sqrt{\frac{D_0}{\bar{m}}} \left(\frac{1}{a^2} + \frac{1}{b^2} \right) t \right], \\
 \dot{w}(t) &= -0.01 \left[\pi^2 \sqrt{\frac{D_0}{\bar{m}}} \left(\frac{1}{a^2} + \frac{1}{b^2} \right) t \right] \sin \left[\pi^2 \sqrt{\frac{D_0}{\bar{m}}} \left(\frac{1}{a^2} + \frac{1}{b^2} \right) t \right], \\
 \ddot{w}(t) &= -0.01 \left[\pi^2 \sqrt{\frac{D_0}{\bar{m}}} \left(\frac{1}{a^2} + \frac{1}{b^2} \right) t \right]^2 \cos \left[\pi^2 \sqrt{\frac{D_0}{\bar{m}}} \left(\frac{1}{a^2} + \frac{1}{b^2} \right) t \right],
 \end{aligned}
 \tag{31}$$

where \bar{m} is the mass of unit area of the plate.

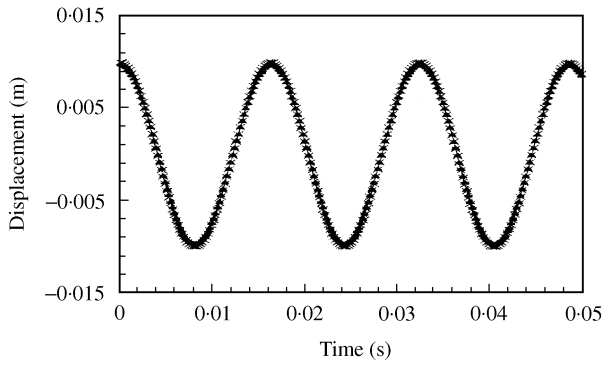


Figure 11. Displacement at the center of the simply supported square plate. \blacktriangle The proposed method; \times exact solution.

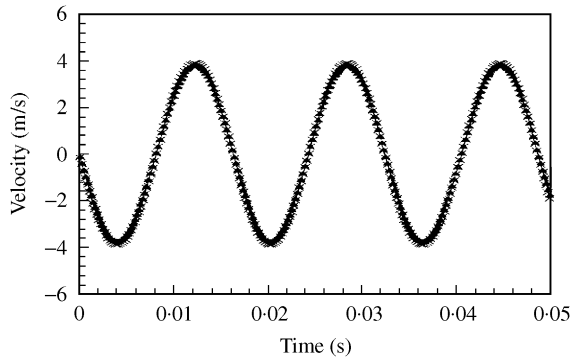


Figure 12. Velocity at the center of the simply supported square plate. \blacktriangle The proposed method; \times exact solution.

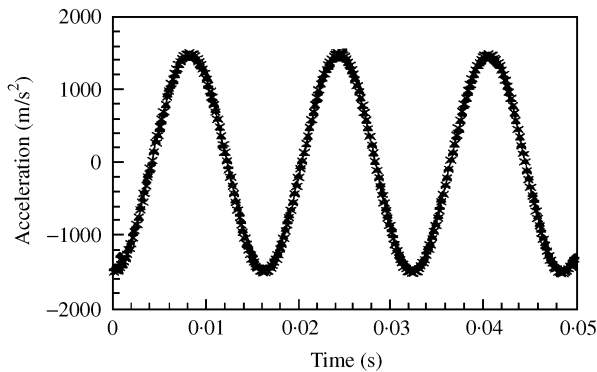


Figure 13. Acceleration at the center of the simply supported square plate. \blacktriangle The proposed method; \times exact solution.

Using $\Delta t = 0.0001$ s, and 500 time steps, the response of the plate is obtained numerically. Figures 11–13 show the variations of the displacement, velocity and acceleration at the center of the plate obtained by the proposed method and the analytical solutions. It can be seen that the present results are satisfactory.

8. CONCLUSIONS

The meshless method, based on the moving least-squares approach, is developed for the dynamic analyses. The boundary conditions are imposed by the penalty method that is a direct method for imposing the boundary conditions. Such an approach does not increase the number of unknowns, and therefore, the computer time will not be very much increased.

A parametric study on the parameters defining the weight function has been carried out and their best values are determined numerically.

The modal analysis of the free vibration and the dynamic response of the forced vibration have been studied. The examples quoted in this paper show that the proposed meshless method is an accurate and efficient one. It is anticipated that the method can be extended to the dynamic analysis of the other structures, such as shells and 3-D structures.

ACKNOWLEDGMENTS

The financial support from The University of Hong Kong is greatly appreciated. The authors are also grateful to the reviewers of the manuscript for their valuable comments and advise.

REFERENCES

1. L. B. LUCY 1977 *The Astronomy Journal* **8**, 1013–1024. A numerical approach to the testing of the fission hypothesis.
2. B. NAYROLES, G. TOUZOT and P. VILLON 1992 *Computational Mechanics* **10**, 307–318. Generalizing the finite element method: diffuse approximation and diffuse elements.
3. T. BELYTSCHKO, Y. Y. LU and L. GU 1994 *International Journal for Numerical Methods in Engineering* **37**, 229–256. Element-free Galerkin methods.
4. T. BELYTSCHKO, Y. KRONGAUZ, D. ORGAN, M. FLEMING and P. KRYSL 1996 *Computer Methods in Applied Mechanics and Engineering* **139**, 3–47. Meshless methods: an overview and recent developments.
5. W. K. LIU, Y. CHEN, C. T. CHANG and T. BELYTSCHKO 1996 *Computational Mechanics* **18**, 73–111. Advances in multiple scale kernel particle methods.
6. C. A. DUARTE and J. T. ODEN 1996 *Numerical Methods for Partial Differential Equations* **12**, 673–705. H-p clouds—an h-p meshless method.
7. J. T. ODEN, C. A. DUARTE and O. C. ZIENKIEWICZ 1998 *Computer Methods in Applied Mechanics and Engineering* **153**, 117–126. A new cloud-based hp finite element method.
8. S. N. ATLURI and T. ZHU 1998 *Computational Mechanics* **22**, 117–127. A new meshless local Petrov–Galerkin (MLPG) approach in computational mechanics.
9. I. BABUSKA and J. M. MELENK 1997 *International Journal for Numerical Methods in Engineering* **40**, 727–758. The partition of unity method.
10. J. M. MELENK and I. BABUSKA 1996 *Computer Methods in Applied Mechanics and Engineering* **139**, 289–314. The partition of unity finite element method: basic theory and application.
11. T. STROUBOULIS, I. BABUSKA and K. COPPS 2000 *Computer Methods in Applied Mechanics and Engineering* **181**, 43–69. The design and analysis of the generalized finite element method.
12. E. ONATE, S. IDELSOHN, O. C. ZIENKIEWICZ and R. L. TAYLOR 1996 *International Journal for Numerical Methods in Engineering* **39**, 3839–3866. A finite point method in computational mechanics—applications to convective transport and fluid flow.
13. T. ZHU, J. ZHANG and S. N. ATLURI 1999 *Engineering Analysis with Boundary Elements* **23**, 375–389. A meshless numerical method based on the local boundary integral equation (LBIE) to solve linear and non-linear boundary value problems.
14. T. BELYTSCHKO, L. GU and Y. Y. LU 1994 *Modeling and Simulation in Materials Science and Engineering* **2**, 519–534. Fracture and crack growth by element-free Galerkin methods.
15. L. W. CORDES and B. MORAN 1996 *Computer Methods in Applied Mechanics and Engineering* **139**, 75–89. Treatment of material discontinuity in the element-free Galerkin method.

16. Y. XU and S. SAIGAL 1998 *Computational Mechanics* **22**, 255–265. Element free Galerkin study of steady quasi-static crack growth in plane strain tension in elastic-plastic materials.
17. P. KRYSL and T. BELYTSCHKO 1999 *International Journal for Numerical Methods in Engineering* **44**, 767–800. The element-free Galerkin method for dynamic propagation of arbitrary 3-D cracks.
18. P. KRYSL and T. BELYTSCHKO 1996 *Computational Mechanics* **17**, 26–35. Analysis of thin plates by the element-free Galerkin method.
19. P. KRYSL and T. BELYTSCHKO 1996 *International Journal of Solid and Structures* **33**, 3057–3080. Analysis of thin shells by the element-free Galerkin method.
20. O. GARCIA, E. A. FANCELLO, C. S. de BARCELLOS and D. C. ARMANDO 2000 *International Journal for Numerical Methods in Engineering* **47**, 1381–1400. hp-clouds in Mindlin's thick plate model.
21. S. H. LEE, H. J. KIM and S. JUN 2000 *Computational Mechanics* **26**, 376–387. Two scale meshless method for the adaptively of 3-D stress concentration problems.
22. W. BARRY and S. SAIGAL 1999 *International Journal for Numerical Methods in Engineering* **46**, 671–693. A three-dimensional element-free Galerkin elastic and elastoplastic formulation.
23. N. H. KIM, K. K. CHOI, J. S. CHEN and Y. H. PARK 2000 *Computational Mechanics* **25**, 157–168. Meshless shape design sensitivity analysis and optimization for contact problem with friction.
24. P. J. S. CHEN and C. H. WU 1998 *Rubber Chemistry and Technology* **71**, 191–213. Application of reproducing kernel particle methods to large deformation contact analysis of elastomers.
25. S. JUN and S. IM 2000 *Computational Mechanics* **25**, 257–266. Multiple-scale meshfree adaptivity for the simulation of adiabatic shear band formulation.
26. E. HARDEE, K. H. CHANG, I. GRINDEANU, S. YOON, M. KANEKO and J. S. CHEN 1999 *Advances in Engineering Software* **30**, 191–213. Structural nonlinear analysis workspace (SNAW) based on meshless methods.
27. S. JUN and W. K. LIU 1998 *International Journal for Numerical Methods in Engineering* **41**, 137–166. Explicit reproducing kernel particle methods for large deformation problems.
28. Y. Y. LU, T. BELYTSCHKO and M. TABBARA 1995 *Computer Methods in Applied Mechanics and Engineering* **126**, 131–153. Element-free Galerkin method for wave propagation and dynamic fracture.
29. T. NAGASHIMA 1999 *International Journal for Numerical Methods in Engineering* **46**, 341–385. Node-by-node meshless approach and its applications to structural analyses.
30. W. K. LIU, S. JUN and Y. F. ZHANG 1995 *International Journal for Numerical Methods in Engineering* **38**, 1655–1679. Reproducing kernel particle methods for structural dynamics.
31. A. E. OUATOUATI and D. A. JOHNSON 1999 *International Journal for Numerical Methods in Engineering* **46**, 1–27. New approach for numerical modal analysis using the element-free method.
32. X. ZHANG, X. LIU, M. W. LU and Y. CHEN 2001 *Communications in Numerical Methods in Engineering* **17**, 165–178. Imposition of essential boundary conditions by displacement constraint equations in meshless methods.
33. P. LANCASTER and K. SALKAUKAS 1981 *Mathematics of Computation* **37**, 141–158. Surfaces generated by moving least-squares method.
34. T. BELYTSCHKO, Y. Y. LU and L. GU 1995 *International Journal for Numerical Methods in Engineering* **32**, 2547–2570. Crack propagation by element-free Galerkin method.
35. O. C. ZIENKIEWICZ 1977 *The Finite Element Method*. New York: McGraw-Hill.
36. W. D. LI 2000 *Ph.D. Thesis Huazhong University of Science and Technology, Wuhan, China*. Theoretical study and engineering application of meshless method (in Chinese).
37. K. J. BATHE 1989 *Finite Element Procedures in Engineering Analysis*. Englewood Cliffs, NJ: Prentice-Hall.
38. B. AKESSON, H. TAGNFORS and O. JOHANESSON 1992 *Charts and Tables in the Area of Structural Vibrations* (in Chinese, translated from Swedish). Beijing: Press of Mechanical Engineering.
39. H. J. FLETCHER, N. WOODFIELD and K. LARSEN 1956 *Natural Frequencies of Plates with Opposite Edges Supported*, AD 107224.
40. R. W. CLOUGH and J. PENZIEN 1975 *Dynamics of Structures*. New York: McGraw-Hill.
41. Z. L. XU 1981 *Elasticity*. Beijing: Higher Education Press; third edition (in Chinese).